JOURNAL OF BIOMEDICAL OPTICS 3(1), 7–11 (JANUARY 1998)

# SIMULTANEOUS MEASUREMENT OF DISPERSION, SPECTRUM, AND DISTANCE WITH A FOURIER TRANSFORM SPECTROMETER

**Thomas Hellmuth and M. Welle**
Fachhochshule Aalen, Studiengang Optoelectronik, Heinrich Rieger Strasse 22/1, 73430 Aalen, Germany

(Paper JBO/IB-006 received July 30, 1997; revised manuscript received Oct. 28, 1997; accepted for publication Nov. 12, 1997.)

## ABSTRACT

A Fourier transform spectrometer is used to simultaneously measure distance, dispersion and spectrum. It is shown that short coherence interferometry has the potential to measure the three-dimensional distribution of the spatial structure of a sample with a resolution determined by the coherence length of the light source, absorption spectrum with a resolution of 1 $cm^{-1}$ and a dispersion with a resolution of up to $10^{-5}$. © *1998 Society of Photo-Optical Instrumentation Engineers.* [S1083-3668(98)01101-0]

**Keywords** Fourier, dispersion, short coherence interferometry.

## 1 INTRODUCTION

Fourier transform spectrometers (FTS) are primarily used in the infrared (IR) and near infrared (NIR) spectral region to record spectra in reflection or transmission mode. The advantage of this type of spectrometer is threefold compared with monochromators.[1] An FTS records all wavelengths of the spectrum simultaneously (Fellgett advantage). A monochromator scans the spectrum sequentially, utilizing only a fraction of the incident light and requiring a much longer acquisition time. Furthermore, simultaneous acquisition with a grating spectrometer is only straightforward in the visible region, where detector arrays are available at reasonable costs. Another aspect is the Jacquinot advantage. An FTS has a circular symmetric optical geometry that is better adapted to typical source geometries than grating spectrometers using slit geometries as entrance and exit diaphragms.

In this paper we discuss a modification of an FTS that allows one to simultaneously measure the absorption spectrum, dispersion, and the thickness of a sample. Dispersion can be measured by beam deviation.[2] Other approaches are critical angle measurements[3] and reflectometry.[4] Information on dispersion of the object can also be derived from an FTS signal with the Kramers–Kronig relation if there are significant absorption lines or bands in the sample spectrum. The method fails for highly transparent media. Our technique is based on measuring the broadening of the interference signal of the FTS caused by the dispersion of the sample.

The setup also allows measurement of the thickness and distance of a reflecting sample. Closely related to our technique is optical coherence tomography (OCT) obtained, for example, with a dual beam interferometer,[5] or a fiber optic Michelson interferometer.[6] These techniques, which are also based on short coherence interferometry, provide information on distances. In principle these techniques also have the capability to provide information on dispersion and spectrum of the sample. However, in order to achieve a high spectral resolution on the order of at least 1 $cm^{-1}$ over a broad spectral range of several thousand wave numbers, all the technical features of an FTS have to be incorporated into an OCT measurement device. For that reason we decided to base our experimental setup directly on an FTS. We want to show in this article that short coherence interferometry, and in particular OCT, have the potential to simultaneously gather information on the spatial distribution of material density, spectral absorption, and dispersion properties of a sample. These are of importance for the identification of substances within tissues and therefore for the functional diagnosis of diseases.[7]

## 2 EXPERIMENTAL SETUP

The setup is shown in Figure 1. It consists of a Bruker Equinox 55 FT spectrometer with a halogen lamp and a silicon detector diode. The FTS can also be described as a Michelson interferometer with a moving reference mirror and a stationary second mirror. The light beam exiting the output port is

Address all correspondence to Thomas Hellmuth. Tel: 497361 568 252; Fax: 497361 568 225; E-mail: thellm@nocws.rzws.fh-aalen.de

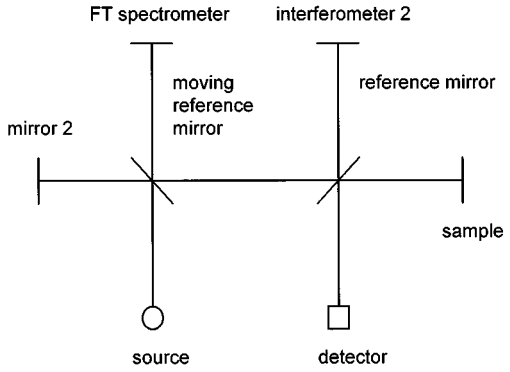


**Fig. 1** Dual Michelson interferometer. The FT spectrometer is in principle a Michelson interferometer with a reference mirror on a moving stage. Interferometer 2 is a Michelson interferometer with a fixed reference mirror and a fixed sample.

coupled into a Michelson interferometer (interferometer 2) consisting of a reference mirror, a beamsplitter cube, and the reflecting sample. The two light beams are superimposed at the detector. The arm lengths of interferometer 2 are deliberately mismatched.

The reference mirror of the FTS moves with constant speed along the reference arm axis of the interferometer. Interference occurs at three moments of the scanning phase of the scanning mirror:

1. The FTS arm length difference matches the arm length difference of the Michelson interferometer.
2. Both arm lengths of the FTS are equal.
3. The negative FTS arm length difference matches the arm length difference of the Michelson interferometer.

One obtains three interference signals. Figure 2 shows the central interference burst and the right satellite peak. The satellite peak on the left side is not shown. Theoretically the central signal (situation 2) is twice as high as the two satellites (situation 1 and 3), as will be shown in Sec. 3. The position of the central peak does not depend on the position of the sample in the second interferometer because it is generated solely by the FTS. The satellite peaks move relative to the central peak when the position of the sample mirror is altered. The distance of the satellites to the central peak is a measure of the sample distance relative to the beamsplitter of the second interferometer. If a dispersive medium is placed in the sample arm of interferometer 2, the satellite signal is broadened because of the wavelength-dependent index of refraction causing a wavelength-dependent delay. The central signal is unaltered because it is generated in the FTS. The degree of the broadening can be utilized to determine the dispersion, as described in the following section.

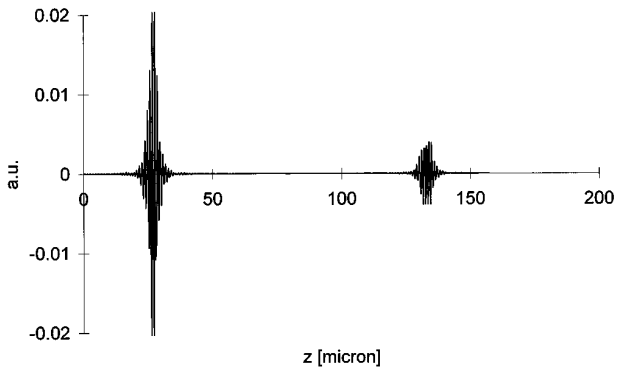


**Fig. 2** Interference signal of the dual Michelson interferometer. The position of the sample mirror does not influence the position of the high peak, but the position of the satellite peak.

## 3 THEORY OF MEASUREMENT

### 3.1 COHERENCE FUNCTION AND INTERFERENCE SIGNAL

The electrical field of the light beam from the light source at a certain position can be described as

$$E(t)=E_0(t)\cdot e^{-i\omega t}.$$

The amplitude $E_0(t)$ is assumed to be complex and stochastic. The power density is

$$I=\frac{1}{2\eta_0}\langle E^*(t)E(t)\rangle \tag{1}$$

$$=\frac{1}{2\eta_0}\lim_{T\to\infty}\frac{1}{2T}\int_{-T}^{T}E^*(t)E(t)dt \tag{2}$$

with the impedance of the vacuum

$$\eta_0=\sqrt{\frac{\mu_0}{\epsilon_0}}=377\ \ \Omega.$$

For simplification we define the normalized amplitude $u(t)=E(t)/\sqrt{2\eta_0}$ so that

$$I=\langle u^*(t)u(t)\rangle.$$

The amplitudes of the two partial beams exiting the FTS are

$$u_1(t)=\tfrac{1}{2}\,u(t) \tag{3}$$

$$u_2(t)=\tfrac{1}{2}\,u(t+\tau_1), \tag{4}$$

where $\tau_1=2\times\Delta z_1/c$. $\Delta z_1$ is the arm length difference of the FTS. The partial waves are further split at the beamsplitter of interferometer 2 so that the amplitude of the beam reaching the detector is

$$u_{\mathrm{det}}(t)=u_{11}(t)+u_{12}(t)+u_{21}(t)+u_{22}(t) \tag{5}$$

with

$$u_{11}(t) = \tfrac{1}{4}\, u(t) \tag{6}$$

$$u_{12}(t) = \tfrac{1}{4}\, u(t+\tau_2) \tag{7}$$

$$u_{21}(t) = \tfrac{1}{4}\, u(t+\tau_1) \tag{8}$$

$$u_{22}(t) = \tfrac{1}{4}\, u(t+\tau_1+\tau_2) \tag{9}$$

and $\tau_2 = 2\times\Delta z_2 / c$ and $\Delta z_2$ as the arm length difference of interferometer 2. Note that $\Delta z_2$, representing the sample distance, is stationary and $\Delta z_1$ changes due to the moving mirror in interferometer 1. For simplicity, all reflectances are assumed to be at unity. The intensity at the detector is:

$$I_{\text{det}}(\tau_1) = \langle |u_{11}(t) + u_{12}(t) + u_{21}(t) + u_{22}(t)|^2 \rangle \tag{10}$$

$$= \tfrac{1}{4}\, I + \tfrac{1}{16}\,[2\cdot(G(\tau_1)+G(\tau_2)) + G(\tau_1+\tau_2) + G(\tau_1-\tau_2)] + \text{c.c.} \tag{11}$$

with the definition of the coherence function

$$G(\tau) = \langle u^*(t)u(t+\tau)\rangle = \lim_{T\to\infty} \frac{1}{2T} \int_{-T}^{T} u^*(t)u(t+\tau)dt$$

and in particular

$$G(0) = \langle u^*(t)u(t)\rangle = I.$$

The coherence time $\tau_c$ is a measure of the length of the interference signal. It is defined as

$$\tau_c = \int_{-\infty}^{+\infty} |g(\tau)|^2 d\tau$$

with the normalized coherence function

$$g(\tau) = \frac{G(\tau)}{G(0)}.$$

If we assume that $\tau_2 \gg \tau_c$ and take into account that $\tau_2$ is constant, we may neglect $G(\tau_2)$ in Eq. (11) so that the result is

$$I_{\text{det}}(\tau_1) = \tfrac{1}{4}\, I + \tfrac{1}{16}\,[2\cdot G(\tau_1) + G(\tau_1+\tau_2) + G(\tau_1-\tau_2)] + \text{c.c.} \tag{12}$$

The signal consists of a time-independent part that is not registered by the ac-coupled detector system and a time-dependent interference term consisting of the central peak $1/8G(\tau_1)$, which is maximum at $\tau_1 = 0$, and two satellite peaks $1/16G(\tau_1+\tau_2)$ and $1/16G(\tau_1-\tau_2)$ with maxima at $\tau_1 = -\tau_2$ and $\tau_1 = \tau_2$. The size of the satellite peaks is half the size of the central peak.

### 3.2 TEMPORAL COHERENCE FUNCTION AND DISPERSION

We assume that a dispersive medium of length $l$ is located in arm 2 of the Michelson interferometer 2. One satellite signal is described by the coherence function:

$$G(\tau_1+\tau_2) = \langle u_1^*(t)u_2(t+\tau_1+\tau_2)\rangle \tag{13}$$

with

$$u_1(t) = \int_{-\infty}^{+\infty} \tilde{u}_1(\nu) e^{i2\pi\nu t} d\nu$$

$$u_2(t) = \int_{-\infty}^{+\infty} \tilde{u}_2(\nu) e^{i2\pi\nu t} d\nu.$$

With dispersion we get:

$$\tilde{u}_2(\nu) = \tilde{u}_1(\nu) e^{i2\pi\,\nu/c\,\Delta n(\nu)2t}.$$

The term $e^{i2\pi\nu/c\Delta n(\nu)2t}$ describes the phase shift each frequency component experiences because of the frequency-dependent part of the index of refraction $\Delta n(\nu)$ of the dispersive medium of length $l$, which describes the difference of the index of refraction between the dispersive sample and air. The total index of refraction of the dispersive medium is $n(\nu) = 1 + \Delta n(\nu)$. The Fourier transform of the coherence function of Eq. (13) is

$$\tilde{G}(\nu) = \tilde{u}_1^*(\nu)\tilde{u}_2(\nu) \tag{14}$$

$$= \tilde{u}_1^*(\nu)\bar{u}_1(\nu) e^{i2\pi\,\nu/c\,\Delta n(\nu)2l} \tag{15}$$

$$= S(\nu) e^{i2\pi\,\nu/c\,\Delta n(\nu)2l} \tag{16}$$

$$= S(\nu)\tilde{H}(\nu). \tag{17}$$

$S(\nu)$ here is the power spectrum of the source and we note that

$$\tilde{G}^*(-\nu) = S(-\nu)\tilde{H}^*(-\nu).$$

We have substituted $e^{i2\pi\nu/c\Delta n(\nu)2l}$ with $\tilde{H}(\nu)$.

## 4 RESULTS AND DISCUSSION

Figure 2 shows the detector signal as a function of $\Delta z_1$ for a mirror sample. The high peak corresponds to $G(\tau_1)$ in Eq. (12); the satellite peak corresponds to $G(\tau_1+\tau_2)$. The power spectrum of each peak is determined by the spectrum of the lamp, the spectral sensitivity of the detector, and the spectrum of the sample reflectivity. With known spectral information on the detector and the lamp, it is possible to determine the absorption of the material. The power spectrum of the peak in Figure 2 is shown in Figure 3.

The theoretically expected ratio of 2 between central and satellite peaks is not achieved because the

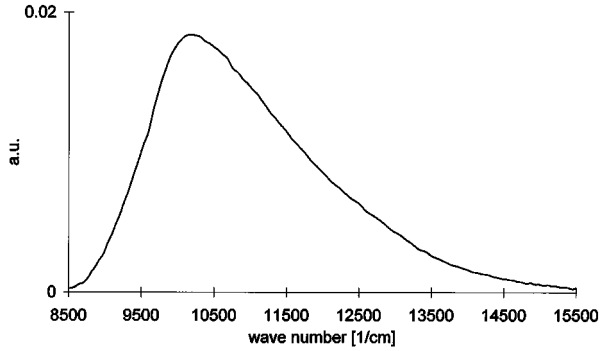


**Fig. 3** Power spectrum of the satellite peak in Figure 2.

size of the light source reduces the interference contrast of the second interferometer. The distance between the central and satellite peaks gives the distance of the sample. The resolution is determined by the coherence length of the light source.

Figure 4 shows the satellite peak when a glass plate (Schott BK7) is placed in one of the arms of the second interferometer. The coherence function is broadened due to dispersion. The frequency-dependent index of refraction causes a delay of each spectral component of the coherence function.

With Eq. (16) the complex spectrum can be described as

$$\tilde{G}(\nu) = S(\nu) e^{i2\pi\nu\,(\Delta n(\nu)2l + z_0)/c} \tag{18}$$

$z_0$ is a fixed offset between the arm lengths of interferometer 2. The modulation period of the spectrum is given by $c/(\Delta n(\nu)2l + z_0)$, which is determined by the fixed offset $z_0$ and a frequency-dependent index of refraction (chirp). The real part of the Fourier-transformed satellite peak of Figure 2 is shown in Figure 5.

One can normalize the function $\bar{G}(\nu)$ in Eq. (18) by dividing it with the power spectrum $S(\nu)$. This is equivalent to dividing the spectrum of Figure 5 by its envelope function. The result is shown in Figure 6.

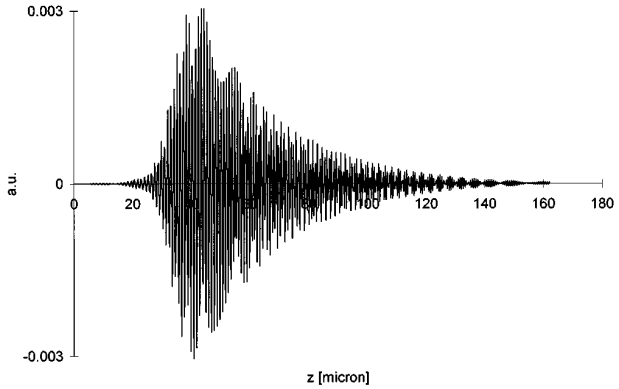


**Fig. 4** Interference signal of the satellite peak with dispersion.

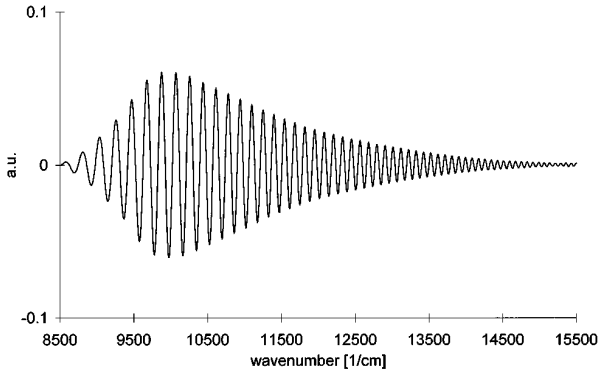


**Fig. 5** Real part of the spectrum of the satellite peak with dispersion.

The modulation frequency is chirped because of dispersion. The frequency is a measure of the delay each spectral component of the coherence function experiences due to the frequency-dependent index of the refraction. In order to obtain the frequency dependence of $\Delta n$, the normalized spectrum in Figure 6 is least-squares fitted with the model function

$$\text{model}(\nu) = \sin\left(2\pi\nu\,\frac{\Delta n(\nu)2l + z_0}{c}\right).$$

The fit parameter function is $\Delta n(\nu)$. One could also calculate $\Delta n(\nu)$ directly from Eq. (16). However, the least-squares fit approach turns out to be more robust for data noise. The thickness $l$ of the sample is determined by measuring the distance of the reflection peaks at the front and rear surfaces of the glass plate. With the index of refraction at $8500\,\text{cm}^{-1}$ (which can be determined iteratively with the experimentally determined dispersion data), one gets the geometrical thickness $l$ of the sample. The fast end of the coherence function on the left in Figure 4 is determined by the fastest frequency component of the spectrum, which is in the case of normal dispersion the short wavelength end of the spectrum in Figure 3. The index of refraction measured as a function of the wavelength and the

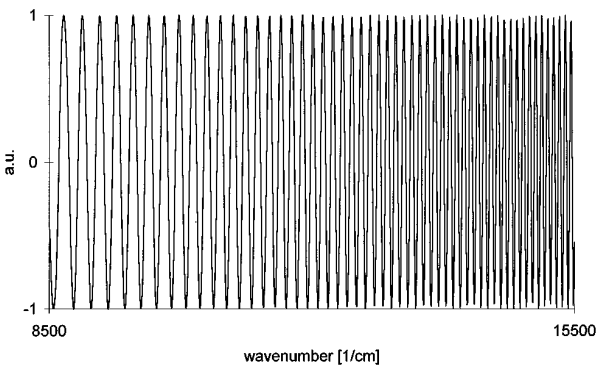


**Fig. 6** Normalized real part of the spectrum of the satellite peak with dispersion.

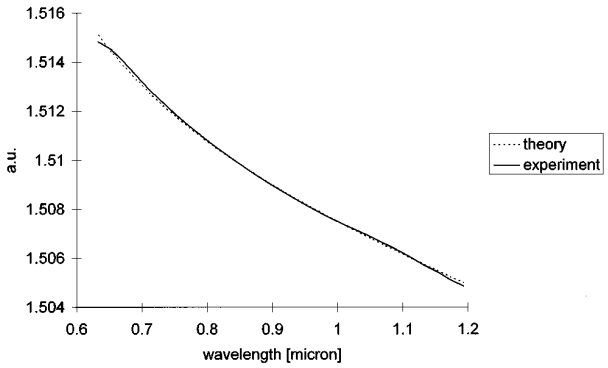


**Fig. 7** Comparison of experimental data and Sellmeier formula for the dispersion curve of BK7.

index curve calculated with the Sellmeier formula for the Schott glass BK7 are shown in Figure 7. Note that the mean deviation of the experimental data from the Sellmeier values is on the order of $10^{-5}$.

## 5 CONCLUSION

The results show that the method described provides spectral and spatial information. In addition, dispersion can be measured. With the current setup, the acquisition time is limited by the light source. For imaging applications, brighter light sources with comparable spectral width are needed. Candidates are, for example, femtosecond or ultrabroad fiber lasers.

## REFERENCES

1. H. A. Gebbie, ''Fourier transform versus grating spectroscopy,'' *Appl. Opt.* **8**, 501 (1969).
2. B. W. Grange, W. H. Stevenson, and R. Viskanta, ''Refractive index of liquid solutions at low temperature: an accurate measurement,'' *Appl. Opt.* **15**(4), 858–859 (1976).
3. S. Sainov and N. Dushkina, ''Simple laser microrefractometer,'' *Appl. Opt.* **29**(10), 1406–1408 (1990).
4. R. M. A. Azzam, ''Explicit determination of the complex refractive index of an absorbing medium from reflectance measurements at and near normal incidence,'' *J. Opt. Soc. Am.* **72**(10), 1439–1440 (1982).
5. C. K. Hitzenberger, ''Measurement of corneal thickness by low coherence interferometry,'' *Appl. Opt.* **31**, 6637–6642 (1992).
6. D. Huang, E. A. Swanson, C. P. Lin, J. S. Schuman, W. G. Stinson, W. Chang, M. R. Hee, T. Flotte, K. Gregory, C. A. Puliafito, and J. G. Fujimoto, ''Optical Coherence Tomography,'' *Science* **254**, 1178–1181 (1991).
7. L. A. Cassis and R. A. Lodder, ''Near-IR imaging of atheromas in living arterial tissue,'' *Anal. Chem.* **65**, 1247 (1993).